Process Parameters Effect on Mechanical Properties and Fatigue Behavior of Friction Stir Weld AA6060 Joints

M. Longo
e-mail: michela.longo@unibg.it

G. D'Urso
e-mail: durso@unibg.it

C. Giardini
e-mail: claudio.giardini@unibg.it

Department of Design and Technologies,
University of Bergamo,
Viale Marconi 5,
24044 Dalmine (BG), Italy

E. Ceretti
Department of Mechanical and
Industrial Engineering,
University of Brescia,
Via Branze 38,
25123 Brescia (BS), Italy
e-mail: elisabetta.ceretti@ing.unibs.it

Friction stir welding (FSW) is the most remarkable welding technology that has been invented and developed in the last decade. It is a solid-state welding process in which a rotating tool is driven into the material and translated along the interface of two or more plates. This technology has been successfully used to join materials that are considered difficult to be welded by fusion welding methods. FSW has potentially significant applications in many industrial fields such as aerospace, automotive, and naval industry. Anyway, FSW technology requires a meticulous understanding of the process and consequent mechanical properties of the welds in order to be used in the production of high performance components. The present work deals with an experimental campaign aimed at the evaluation of the mechanical properties of AA6060 T6 friction stir welded joints. The butt joints obtained using two different tool geometries (standard and threaded) were performed by varying the welding parameters, namely, tool rotating speed and feed rate. The standard tool was a very simple device fabricated using AISI 1040 steel, with a flat shoulder and a cylindrical pin. The threaded tool was a more complex device based on two main components: a tool holder, with a flat shoulder, and a threaded probe obtained using a commercial thread forming tap. The quality of the joints was evaluated in terms of both tensile strength (UTS) and fatigue behavior. The study of axial pulsing fatigue properties required the fabrication of a specific testing device able to avoid parasite bending moments. In order to estimate the more efficient and effective tool type, the welding forces (axial and longitudinal) were also measured. [DOI: 10.1115/1.4005916]

Keywords: FSW, aluminum, butt joints, mechanical properties, welding forces, fatigue behavior

1 Introduction

FSW is a solid-state welding process first introduced by The Welding Institute (TWI) in Cambridge (UK) and patented by Thomas et al. [1,2]. In this welding process, a rotating tool is driven into the material and translated along the interface of two or more plates. Friction heats the material which is extruded around the tool and forged by the large pressure produced by the tool shoulder.

Amongst several research papers dealing with the positive aspects of this technology, Peel et al. [3] evidenced how FSW may offer several advantages such as, high quality joints, precise external control and high levels of repeatability, no need of special preparation of the samples, low energy process requirements, and low creation of waste or pollution. Furthermore, this technology is suitable for aluminum alloys considered difficult to be welded by conventional welding technologies or even for dissimilar alloys. Moreover, compared to traditional welding techniques, the joint is obtained through the deformation of the material at temperatures below the melting point, so reducing problems related to distortions and residual stresses. For all the above mentioned reasons, this technique has potentially significant applications in automotive, aerospace, and naval industries.

Anyway, FSW technology requires a meticulous understanding of the process and consequent mechanical properties of the welds in order to be used in the production of high performance components, especially in aerospace where, as highlighted in Bussu and Irving [4], damage tolerance design is used extensively in aircraft construction and is mandatory for large civil aircrafts.

Many studies conducted on FSW of aluminum alloys, and, in particular, Dubourg et al. [5] showed how the process parameters can affect the welding conditions and the weld properties: rotational speed and feed rate, tool geometry, and position of the pin axes were investigated in order to obtain high quality welds. Cavaliere et al. [6] studied the effects of welding parameters on mechanical properties of AA6056 joints, showing how the welding speed influences the fatigue behavior. Also Lakshminarayanan and Balasubramanian [7] studied the effect of process parameters on the UTS of friction stir welded RDE-40 aluminum alloy applying the Taguchi method for process parameters optimization.

It is important to remark how the fatigue resistance is strictly related to residual stress and thermal load: Buffa et al. [8] studied this aspect showing how the residual stresses are mainly due to the thermal flux generated by the frictional forces especially acting at the shoulder-workpiece interface.

Rotational speed has been identified as one of the most significant process variable: high rotational speeds may raise the strain rate, so influencing the recrystallization process. Moreover, Lomolino et al. [9] showed how high welding speeds are related to low heat inputs, which result in faster cooling rates of the welded joint. This can significantly reduce the extent of metallurgical transformations taking place during welding (such as solubilization, reprecipitation, and coarsening of precipitates) and hence the local strength of individual regions across the weld zone.

Buffa et al. [10], studying the tool geometry (shoulder and pin) influence, showed how it is a key aspect to assure a good quality

Contributed by the Materials Division of ASME for publication in the JOURNAL OF ENGINEERING MATERIALS AND TECHNOLOGY. Manuscript received June 23, 2011; final manuscript received December 30, 2011; published online March 26, 2012. Assoc. Editor: Pedro Peralta.

weld and to reduce the load during the process. In particular, the tool shoulder represents the main source of heat generation during the process and the constraint to material expulsion; at the same time, the pin is the source for material deformation and heat generation in the nugget. Also Elangovan et al. [11] conducted an extensive research studying the influence of tool pin profile on friction stir welded AA6061 aluminum alloys. Okada et al. [12] evidenced how the mechanical properties of a friction stir welded aluminum alloy are directly related to the material flow, which occurs around the tool and then related to the tool shape.

An important parameter in FSW is the ratio of dynamic volume (the volume swept by the pin during rotation) to static volume (that is the volume of the pin itself). As affirmed by Dubourg and Dacheux [13], increasing this ratio results in a reduction in the formation of voids in the welds and allows the surface oxide to be more effectively disrupted and dispersed within the microstructure. In conventional FSW, the dynamic/static ratio can be increased by using re-entrant features, flutes, threads, or flats machined into the pin. Anyway, an optimal tool shape and the real effectiveness of some tool profiles are still a matter of debate. The effective tool shape for a specific application seems to be dependent on both the material to be welded and the joint configuration (butt, lap, T-joint, etc.). Prado et al. [14,15] showed that, in some cases, even starting from a threaded pin, due to tool wear, a threadless but still effective pin shape is reached after a short welding time. Lorrain et al. [16] confirmed the same hypothesis.

The tool geometry may also influence the welding forces that represent another important aspect for the production of a high quality joint. Hosein et al. [17] and Kumar and Satish [18] investigated the role of axial forces on the mechanical properties of the joints finding out optimal force values for producing defect-free welds.

Ericsson and Sandström [19] evidenced how another important aspect for FSW joints is their fatigue behavior, especially for aircraft and automotive components, comparing the behavior of both conventional and friction stir welding technologies.

In the last few years, many efforts were carried out to investigate the fatigue properties of friction stir welded joints and how they can be related to the process that has been carried out. In particular, James et al. [20] deeply analyzed the influences of process parameters, welding defects, and residual stress on the fatigue behavior. However, the fatigue strength in FSW is a not completely established aspect because of the complexity of the process and the relatively new joining technology, and this topic is still matter of study. In fact, although the range of friction stir welding parameters is generally wide and the macroscopic defects such as flaws, porosity, and lack of bonding are rarely produced, the general fatigue evaluation of friction stir welded joints and components is still not well-known and especially the influence of various defects in the friction stir welded joints on the fatigue behavior is still uncertain. In particular, some researches (such as Shusheng et al. [21]) showed that a special defect referred to a "zigzag-curve" defect will be produced across the whole section of stir zone even if the better optimized welding parameters are employed. Moreover, during FSW processing, the initial oxide layer is broken up and distributed locally on the final butt face of the cross-section.

Other efforts were made by Dickerson and Przydatek [22] and Fratini et al. [23] for the definition of specific testing methods for friction welded joints. This aspect is particularly important if we consider that the general fatigue design and assessment specification for friction stir welded joints and components are not fully recommended and the current fatigue design standards, based on fusion welded joints (such as IIW and Eurocode 9) are hardly suitable for FSW component fatigue design, since the fatigue properties of FSW joints are in general higher than the characteristics of fusion welded joints [21].

The present study deals with the results of an experimental campaign aimed at the evaluation of mechanical properties of AA6060 friction stir welded butt joints. In particular, the joints obtained by using two different tool geometries and different working parameters, according to a suitable design-of-experiments, were characterized in terms of both UTS and fatigue behavior by means of the analysis of variance (ANOVA) technique. Welding forces, as a function of the above mentioned parameters, were also measured and are reported in the present paper.

2 Experimental Campaign

2.1 Friction Stir Welding Campaign. The experimental campaign was performed by means of a computer numerical control (CNC) machine tool. Butt joints were carried out on sheets having a thickness of 5 mm. An aluminum alloy AA6060 (Al-Mg-Si-Cu) in the artificially aged condition T6 was considered for this purpose. The mechanical properties of the base material are reported in Table 1. Several welding operations were carried out

Table 1 Mechanical properties of the base material (AA 6060 T6)

UTS (MPa)	Yield strength (MPa)	Elongation at break
215	182	18%

Table 2 Experimental plan

Tool rotational speed (S) (rpm)	Feed rate (f) (mm/min)	Tool type
1000, 1500, 2000	150, 300, 600	Standard, Threaded

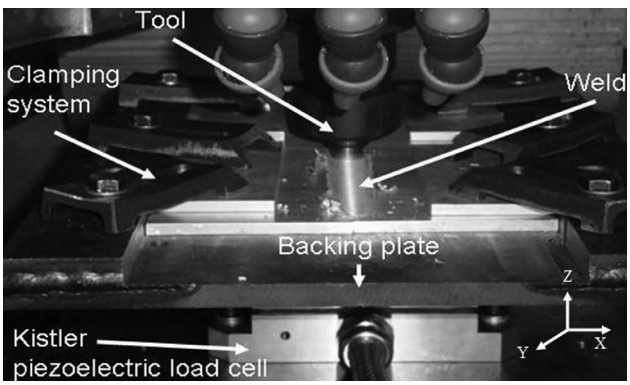

Fig. 1 Details of both experimental setup and force measuring system

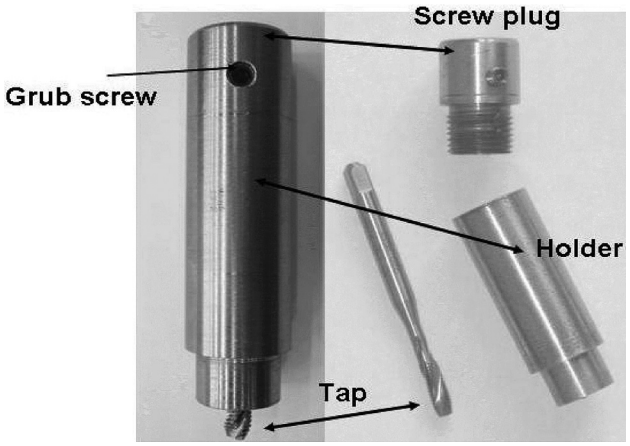

Fig. 2 Details of the threaded tool

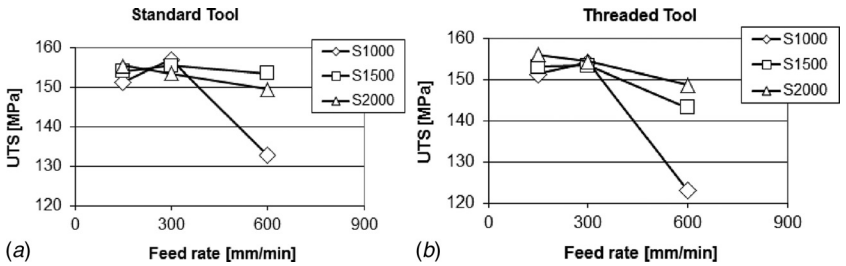

Fig. 3 UTS as function of feed rate and rotational speed for both (*a*) standard and (*b*) threaded tools

Table 3 UTS as function of feed rate and rotational speed

	Speed (rpm)	Feed (mm/min)	UTS (MPa)		Speed (rpm)	Feed (mm/min)	UTS (MPa)
Standard tool	1000	150	151.3	Threaded tool	1000	150	151.2
		300	156.8			300	154.0
		600	132.6			600	123.0
	1500	150	154.0		1500	150	152.9
		300	155.4			300	153.2
		600	153.4			600	143.1
	2000	150	155.4		2000	150	156.0
		300	153.5			300	154.4
		600	149.4			600	148.6

by varying process parameters, namely, tool rotational speed and feed rate and by using two different tool geometries. In particular, both standard and threaded tools were taken into account. All the welding conditions are reported in Table 2. These conditions were adopted for both standard and threaded tools, for a total amount of 18 different welding conditions; five repetitions were carried out for each combination of parameters. The same tilt angle, equal to 2.5 deg, was assumed for all the experiments while the distance between the tool tip and the baking plate (clearance) was always set equal to 0.2 mm.

A Kistler piezoelectric load cell was used to measure the welding forces in the main directions and the corresponding data were recorded. Figure 1 shows some details of the experimental setup.

2.2 Tools Description. A standard tool with smooth plane shoulder and cylindrical pin were fabricated using AISI 1040 steel; shoulder and pin diameters were, respectively, equal to 15 and 5 mm. The threaded tool employed for this work was fabricated taking as a starting point a study described in Nishihara [24]. Based on this idea, a new tool was developed using four distinct components: a commercial M5 thread forming tap, a holder with flat shoulder, a screw plug, and a grub screw (Fig. 2). The holder, with a shoulder diameter equal to 15 mm, was made using AISI 1040 steel. The holder was hollowed and tapped inside (the threads were only executed in correspondence of the shoulder, in the bottom part of the cylinder) to be coupled together with the forming tap. This solution was applied to register the axial position of the tap and to face the axial force during welding. A screw plug was screwed on the top part of the holder; during the welding process, the connection between the holder and the plug was guaranteed by the collet chuck used to couple the tool with an ISO40 shank for milling machine. A small tapped hole through the screw plug was used to guarantee the torque moment transmission by means of a grub screw.

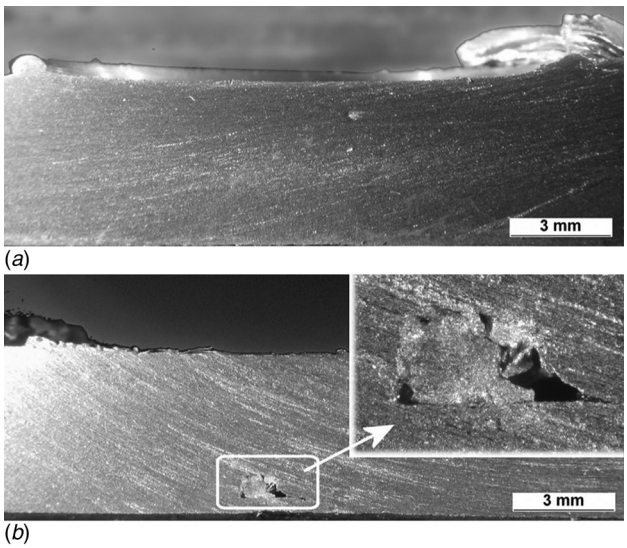

Fig. 4 Comparison between a sound welded section (*a*) and a section with tunnel (*b*)

3 Tensile Tests and Welding Forces

3.1 Experimental Devices and Procedure. A universal testing machine Galdabini with a load cell of 50 kN was employed to evaluate the tensile properties of the friction stir welded joints as a function of the different process parameters for both the adopted tools. Specimens with a section of about 125 mm^2 (width equal to 25 mm) were obtained from the welded plates. The mechanical properties of the welded joints were investigated along a direction orthogonal to the welding path. In all cases, tests were executed assuming a tensile direction parallel to the rolling direction of the

Table 4 Analysis of variance for UTS, P-value data

Source	P-value
Tool	0.030
Speed (rpm)	0
Feed (mm/min)	0
Speed × feed (mm/min)	0
Tool × speed (rpm)	0.235
Tool × feed (mm/min)	0.075
Tool × speed (rpm) × feed (mm/min)	0.8

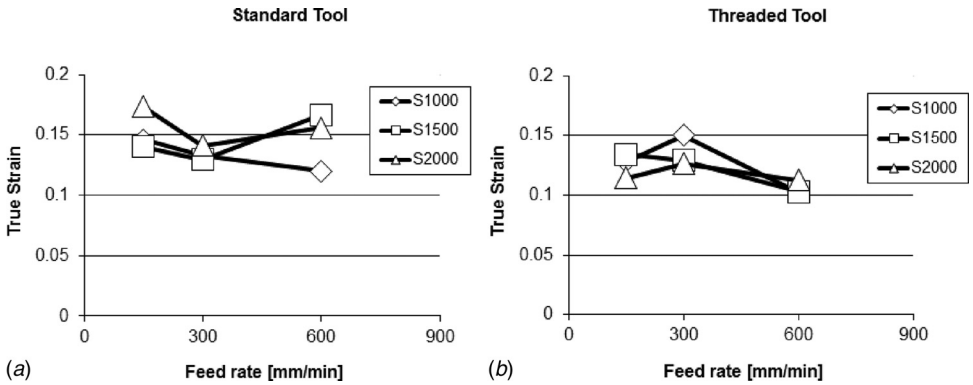

Fig. 5 Strain in correspondence of the UTS as a function of feed rate and rotational speed for both (*a*) standard and (*b*) threaded tools

Table 5 Strain in correspondence of the UTS

	Speed (rpm)	Feed (mm/min)	True strain		Speed (rpm)	Feed (mm/min)	True strain
Standard tool	1000	150	0.15	Threaded tool	1000	150	0.13
		300	0.13			300	0.15
		600	0.12			600	0.10
	1500	150	0.14		1500	150	0.13
		300	0.13			300	0.13
		600	0.17			600	0.10
	2000	150	0.17		2000	150	0.11
		300	0.14			300	0.13
		600	0.16			600	0.11

Table 6 Analysis of variance for strain, P-value data

Source	P-value
Tool	0
Speed (rpm)	0.359
Feed (mm/min)	0.05
Speed × feed (mm/min)	0.052
Tool × speed (rpm)	0.007
Tool × feed (mm/min)	0
Tool × speed (rpm) × feed (mm/min)	0.058

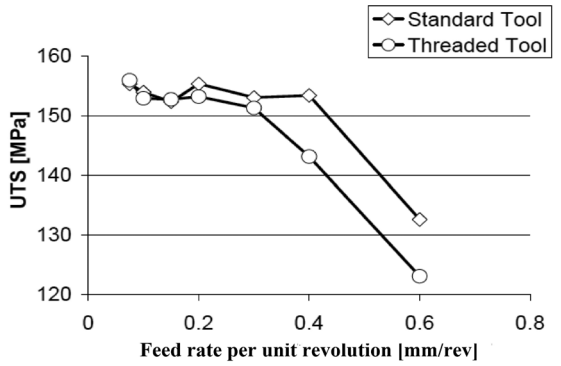

Fig. 6 UTS as function of feed rate per unit revolution (mm/rev) and tool type

aluminum plates. A quite large number of specimens (90 samples) were taken into account: five specimens for each welding condition, obtained using both simple and threaded tools, were tested.

3.2 Preliminary Analysis. Before to carry out the tensile tests, all the welded plates were cut along the transversal section

Table 7 Analysis of variance for UTS, P-value data

Source	P-value
Tool	0.014
Feed rate per unit revolution (mm/rev)	0
Tool × feed rate (mm/rev)	0.168

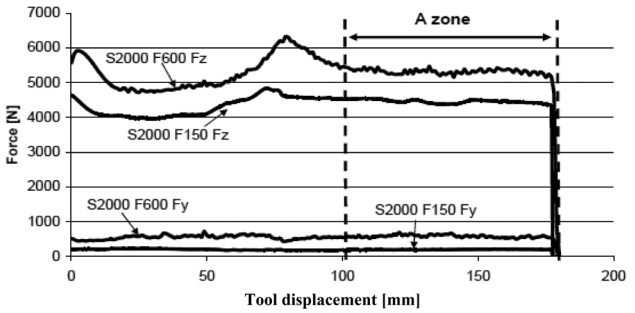

Fig. 7 Welding forces in *Y* and *Z* directions

in order to visually evaluate the quality and the aspect of the joints. According to the literature, four zones were identified: the base material, unaffected by welding, the heat affected zone (HAZ), due to thermal cycle of heating and cooling near the welding, the thermomechanically affected zone (TMAZ), partially recrystallized and modified by severe deformation and heating induced by friction, and the dynamic recrystallization zone , with very fine and homogeneous microstructure. Based on a visual analysis of section macrographs, the nugget appearance resulted to be quite similar for all conditions. A large HAZ was observed in the welding produced with low feed rate, due to the higher heating produced. The presence of voids in TMAZ was observed in some welds obtained using a rotational speed equal to 1000 rpm and a feed rate equal to 600 mm/min (as shown in Sec. 3.3).

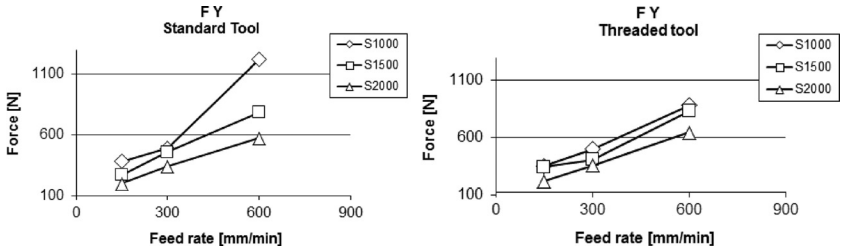

Fig. 8 Average loads as a function of process and tool type for welding force in welding direction (FY)

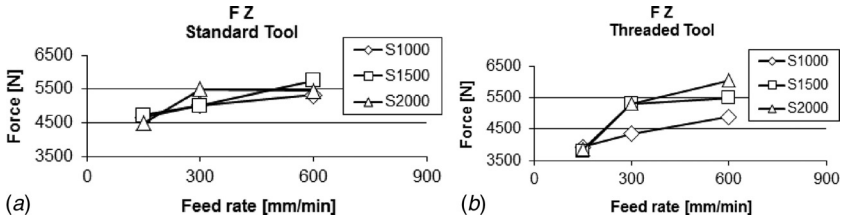

Fig. 9 Average loads as a function of process and tool type for welding force axial direction (FZ)

Table 8 Analysis of variance for average loads FY and FZ, P-value data

Source	*P*-value FY	*P*-value FZ
Tool	0.657	0.071
Speed (rpm)	0.025	0.145
Feed (mm/min)	0.001	0.004
Tool × speed	0.372	0.368
Tool × feed	0.707	0.185
Speed × feed [mm/min]	0.325	0.394

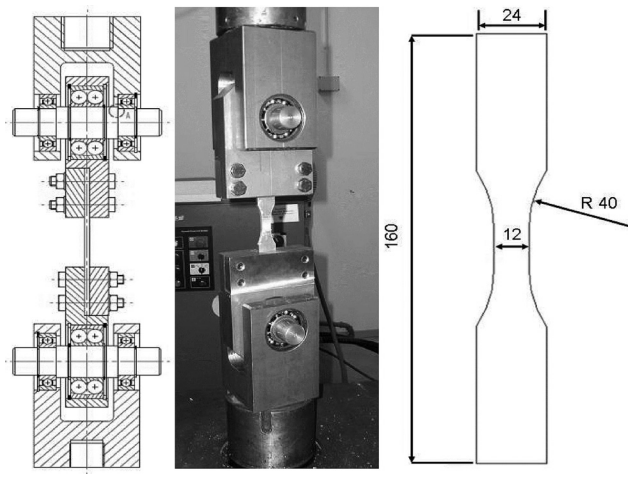

Fig. 10 Details of testing device and specimen geometry

3.3 Results. Figures 3(*a*) and 3(*b*) show the results of the tensile tests campaign as a function of feed rate and speed for both standard and threaded tools. Each marker represents the average stress obtained from five tests. The same results in tabular format are reported in Table 3. Rupture was normally localized in the HAZ on the retreating side. With respect to the basic material UTS (215 MPa), good results in terms of tensile strength and corresponding strain were found for both the tool geometries. The best condition in terms of UTS (163 MPa) was obtained using the threaded tool, a rotational speed equal to 2000 rpm and a feed rate equal to 150 mm/min. The welding efficiency in this case was

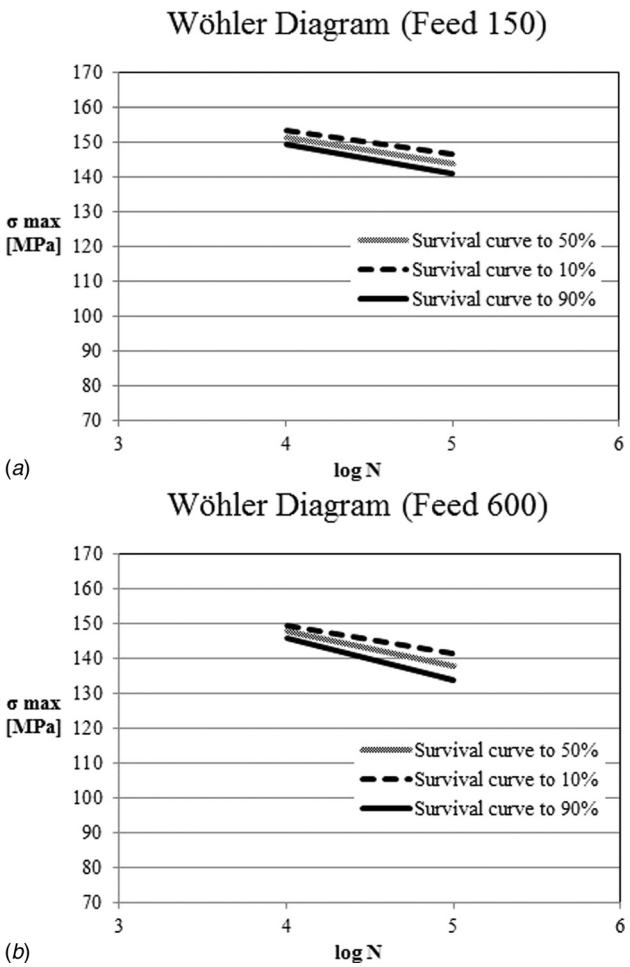

Fig. 11 Wöhler diagram, standard tool, speed 2000 rpm (*a*) feed rate 150 mm/min and (*b*) feed rate 600 mm/min

equal to 76%. The UTS is remarkably lower for $S = 1000$ rpm and $f = 600$ mm/min; this effect may be due to the high feed rate per unit revolution (mm/rev) that gives rise to both a low thermal contribution and a low material mixing resulting in the presence

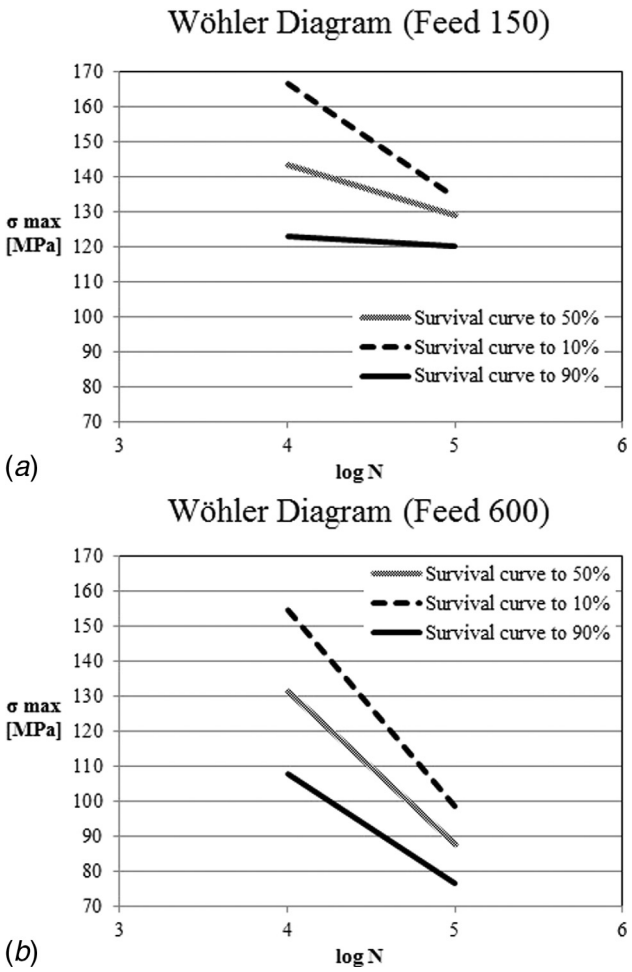

Fig. 12 Wöhler diagram, threaded tool, speed 2000 rpm (*a*) feed rate 150 mm/min and (*b*) feed rate 600 mm/min

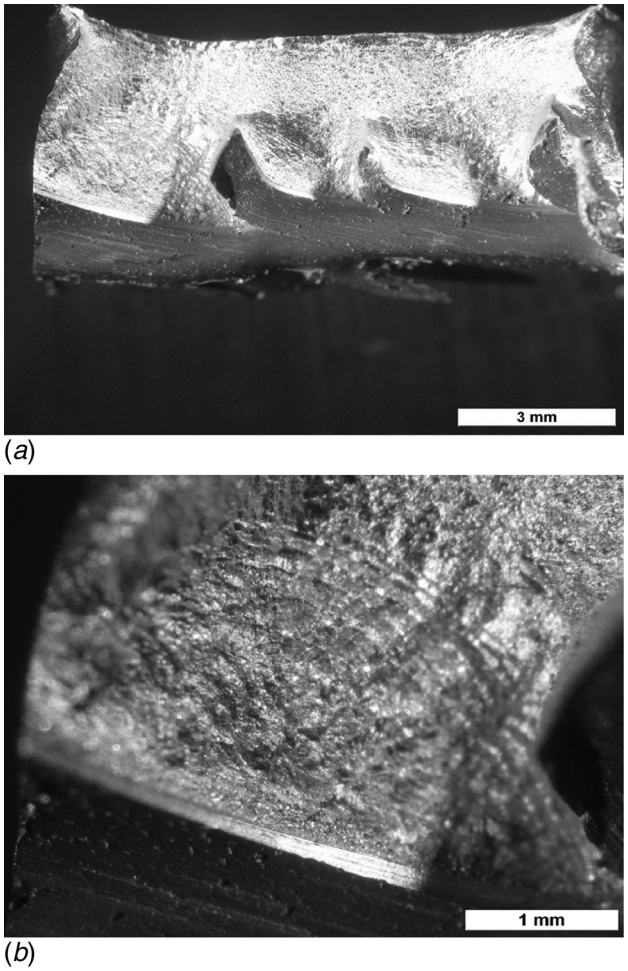

Fig. 13 Fracture surface of the specimen for (*a*) 10^4 and (*b*) 10^5

of voids. In this case, the rupture happened in the TMAZ. Figure 4 shows a comparison between a sound welded section (Fig. 4(*a*)), obtained for $S = 2000$ rpm, $f = 150$ mm/min, and a section with tunnel (Fig. 4(*b*)), obtained for $S = 1000$ rpm, $f = 600$ mm/min).

An ANOVA for UTS data was carried out and the results are resumed in Table 4. A general good repeatability, with low data scatter, was found. Both rotational speed and feed rate resulted to have a significant effect on UTS, while negligible effects can be noticed using different tool geometries.

Figures 5(*a*) and 5(*b*) show the strain values, in correspondence of UTS, as a function of feed rate and rotational speed for both threaded and standard tools. Also in this case, each marker represents the average of the five tests. The same results in tabular format are reported in Table 5. The corresponding ANOVA is resumed in Table 6. Tool resulted to be the most significant parameter affecting the strain, both as single parameter and in combination with feed rate and rotational speed.

In order to evaluate the mixing and thermal effects in the different process conditions, a further analysis for the UTS values was performed representing all data as a function of the feed rate per unit revolution (mm/rev) (Fig. 6). A corresponding ANOVA was also performed (Table 7). UTS resulted to be dependent from this last parameter, while minor effects can be related to the tool shape. A very low UTS for high values of feed rate per unit revolution can be noticed; this is in agreement with the previous hypothesis.

3.4 Welding Forces. The welding forces, measured in the main welding directions, were investigated as a function of welding process parameters and tool shape. Figure 7 shows an example of force diagrams in axial direction (Z) and welding direction (Y) measured using a threaded tool: $S = 2000$ rpm, $f = 150$–600 mm/min.

As a general remark, the force in axial direction (Z) represents the main component of the total force. Furthermore, welding forces differ significantly by varying the process parameters (namely, tool rotational speed and feed rate). A single scalar, corresponding to the average force, was extracted from each curve in order to compare the results obtained in all the testing conditions.

Table 9 Fatigue limits for a survival probability of 50%

Tool	Feed (mm/min)	σd (10^4 cycles) (MPa)	Deviation (s) (MPa)	σd (10^5 cycles) (MPa)	Deviation (s) (MPa)
Standard	150	151.3	1.5	143.8	2.8
Standard	600	147.5	1.7	137.5	3
Threaded	150	143	18	129	4
Threaded	600	131	18	88	9

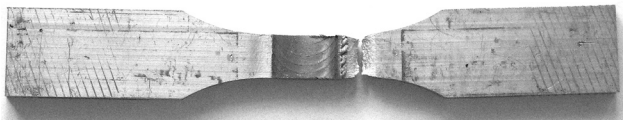

Fig. 14 Example of fracture location on a specimen

The average values were calculated in the second half of the tool path (A zone, Fig. 7), where steady state conditions can be assumed. The diagrams reported in Figs. 8 and 9 show, respectively, the average loads in *Y* and *Z* directions as a function of the process parameters for both threaded and standard tools.

The corresponding ANOVA results are reported in Table 8. With regard to the tool type, no influence can be observed for both welding force in the welding direction (FY) and the welding force axial direction (FZ). The rotational speed only affects FY values, while the most influencing factor resulted to be the feed rate. The ANOVA does not show any interaction effect between the parameters.

4 Fatigue Behavior

4.1 Experimental Tests. The fatigue behavior of the joints at 10^4 and 10^5 cycles was also investigated by means of the stair case method. The tests were executed using a universal testing machine Instron with a 25 kN load cell. A specific testing device was designed and fabricated for this purpose (Fig. 10). The main characteristics of the system are reported below:

- Unlimited fatigue life
- Maximum testing load 17 kN
- Spherical hinges for avoiding parasite bending moments
- Light weight to reduce inertia effects

The specimen dimensions were selected by combining the literature data and limits of the testing device. The thickness was maintained equal to the original sheet thickness and a particular attention was paid in order to leave the welded surface unchanged; the length was chosen in order to obtain a suitable contact surface between the specimen and the clamping system. Because of the loading limits of the testing device (17 kN), the specimen section was limited to 60 mm^2, so resulting in a specimen width of 12 mm. Specimens were fabricated with a fillet radius equal to 40 mm, in order to achieve a notch coefficient $Kf = 0.1$. This datum was calculated by means of the finite element method (FEM) code ABAQUS.

Axial pulsing tests were carried out at a frequency of 4 Hz; both 10^4 and 10^5 loading cycles were performed. In order to avoid specimen instability, the ratio between the minimum and maximum load *R* was set equal to 0.1. The theoretical fatigue limits were estimated using the Wöhler curves and the Haigh diagrams. It is important to remark that the real axial load required for the tests resulted to be definitely higher than the theoretical loads. Fifteen repetitions were executed in each condition.

4.2 Analysis of the Results. Figure 11 shows the Wöhler diagram of the joints obtained using the standard tool (speed 2000 rpm, feed rate 150–600 mm/min). Figure 12 shows the Wöhler diagram of the joints obtained using the threaded tool (speed 2000 rpm, feed rate 150–600 mm/min). For the sake of completeness, the data referring to the survival probability of 50% at different feed rates are resumed in Table 9.

Some differences in terms of fatigue resistance can be appreciated between the standard and threaded tools. In particular, the joints obtained by using the standard tool seem to have a general higher fatigue resistance with a lower data scatter. Referring to both the tools, it is possible to observe that the fatigue resistance of the joints obtained by using a traverse rate equal to 150 mm/min is higher with respect to the joints obtained by using a welding speed equal to 600 mm/min. This result confirms that the optimal welding conditions in terms of UTS are also the most favorable conditions for the fatigue resistance. Grain size reduction and high strain hardening can be the reasons of this effect. These results can be also due to the surface finishing, in effect the joints welded using low traverse rate show a higher surface quality with respect to the others. In any case, the cracks of the broken specimens always occurred on the retreating side; a different consideration must be done for the specimens unbroken at 10^4 cycles since they often show visible cracks in the middle of the joint. As a final result, it is possible to state that low welding speed may improve the fatigue resistance at both 10^4 and 10^5 cycles.

Moreover, some macrographic analyses were carried out on the broken specimens. The two images reported in Fig. 13 show, respectively, a detail of a cracking surface of a specimen tested at 10^4 and 10^5 cycles. It must be said that all the fatigue cracks are localized outside of the joint line (Fig. 14). The rupture occurred in almost any case in the heat affected zone and broken joints showed two different types of surfaces. In the case of specimens broken at 10^4 cycles, the fracture surface is rough and wrinkled (Fig. 13(*a*)); the maximum load recorded in this case is in fact very close to the specimens fracture limit.

On the opposite, the specimens broken at 10^5 cycles show a clear separation between the area of stable defect propagation and the area subjected to the final rupture. The beach marks, typical of the fatigue crack region, can be noticed in the area characterized by a smooth and bright surface. As shown in the Fig. 13(*b*), fatigue crack region is quite wide representing about the 5% of the total fractured area. The considerable wide rough surface observed in both cases is due to the application of very high testing loads.

5 Conclusion

This study presented the effects of FSW parameters for two different tool geometries. A range of values for feed rate and rotational speed was determined to obtain an acceptable weld quality. Both rotational speed and feed rate resulted to have significant effects on UTS, while nonsignificant differences can be noticed by using the two tested tool geometries.

As a general remark, the threaded tool design for this study proved to be effective in friction stir welding of AA6060 plates even though no significant differences were found in terms of UTS (compared with the standard tool).

The welding forces, measured in the main welding directions, were investigated as functions of process parameters and tool geometry. The feed rate resulted to be the most significant parameter affecting the welding forces and the condition that minimizes the forces in *Z* direction was obtained using the threaded tool.

The fatigue behavior of the joints at 10^4 and 10^5 cycles was also investigated by means of the stair case method. As a general remark, the joints obtained by using the standard tool show a general higher fatigue resistance with a lower data scatter.

References

[1] Thomas, W. M., Nicholas, E. D., Needham, J. C., Murch, M. G., Temple-Smith, P., and Dawes, C. G., 1991, "Friction Stir Butt Welding," GB Patent Application No. 9125978.8, International Patent Application No. PCT/GB92/02203.

[2] Thomas, W. M., Nicholas, E. D., Needham, J. C., Murch, M. G., Temple-Smith, P., and Dawes, C. J., 1995, "Friction Welding," U.S. Patent Application No. 54603176.

[3] Peel, M., Steuwer, A., Preuss, M., and Withers, P. J., 2006, "Microstructure, Mechanical Properties and Residual Stresses as a Function of Welding Speed in Aluminium AA5083 Friction Stir Welds," Proceedings of the 6th International Symposium on Friction Stir Welding, Saint Sauveur, Quebec, Canada.

[4] Bussu, G., and Irving, P. E., 2003, "The Role of Residual Stresses and Heat Affected Zone Properties on Fatigue Crack Propagation in Friction Stir Welded 2024-T352 Aluminium Joints," Int. J. Fatigue, **25**, pp. 77–88.

[5] Dubourg, L., Gagnon, F.-O., Nadeau, F., St-Georges, L., and Jahazi, M., 2006, "Process Window Optimization for FSW of Thin and Thick Sheet Al Alloys Using Statistical Methods," Proceedings of the 6th International Symposium on Friction Stir Welding, Saint Sauveur, Quebec, Canada.

[6] Cavaliere, P., Campanile, G., Panella, F., and Squillace, A., 2006, "Effect of Welding Parameters on Mechanical and Microstructural Properties of AA6056 Joints Produced by Friction Stir Welding," J. Mater. Process. Technol., **180**, pp. 263–270.
[7] Lakshminarayanan, A. K., and Balasubramanian, V., 2008, "Process Parameters Optimization for Friction Stir Welding of RDE-40 Aluminium Alloy Using Taguchi Technique," Trans. Nonferrous Metal Soc. China, **18**, pp. 548–554.
[8] Buffa, G., Fratini, L., Pasta, S., and Shivpuri, R., 2008, "On the Thermo-Mechanical Loads and the Resultant Residual Stresses in Fiction Stir Processing Operations," CIRP Ann. - Manuf. Technol., 57(1), pp. 287–290.
[9] Lomolino, S., Tovo, R., and Dos Santos, J., 2005, "On the Fatigue Behaviour and Design Curves of Friction Stir Butt Welded Al Alloys," Int. J. Fatigue, **27**, pp. 305–316.
[10] Buffa, G., Hua, J., Shivpuri, R., and Fratini, L., 2006, "Design of the Friction Stir Welding Tool Using the Continuum Based FEM Model," Mater. Sci. Eng. A, **419**, pp. 381–388.
[11] Elangovan, K., Balasubramanian, V., and Valliappan, M., 2008, "Influences of Tool Pin Profile and Axial Force on the Formation of Friction Stir Processing Zone in AA6061 Aluminium Alloy," Int. J. Adv. Manuf. Technol., **38**, pp. 285–295.
[12] Okada, T., Kida, K., Iwaki, S., Eguchi, N., Ishikawa, T., Oiwa, N., and Namba, K., 2006, "Studies on Characteristics of Friction Stir Welded Joints in Structural Aluminium Alloys—Part 1: Metallurgical Features of Friction Stir Welded Zone," Proceedings of the 6th International Symposium on Friction Stir Welding, Saint Sauveur, Quebec, Canada.
[13] Dubourg, L., and Dacheux, P., 2006, "Design and Properties of FSW Tools: A Literature Review," Proceedings of the 6th International Symposium on Friction Stir Welding, Saint Sauveur, Quebec, Canada.
[14] Prado, R. A., Murr, L. E., Shindo, D. J., and Soto, K. F., 2001, "Temperature Field in the Vicinity of FSW-Tool During Friction Stir Welding of Aluminum Alloys," Scr. Mater., **45**, pp. 175–180.
[15] Prado, R. A., Murr, L. E., Soto, K. F., and Mc Clure, J. C., 2003, "Characterization of Tool Wear and Weld Optimization in the Friction-Stir Welding of Cast Aluminum 359+20% SiC Metal-Matrix Composite," Mater. Sci. Eng. A, **349**, pp. 156–165.
[16] Lorrain, O., Favier, V., Zahrouni, H., and Lawrjaniec, D., 2010, "Friction Stir Welding Using Unthreaded Tools: Analysis of the Flow," J. Mater. Form, **3**, pp. 1043–1046.
[17] Hosein, A., Dechao, L., and Radovan, K., 2009, "Numerical and Experimental Investigations on the Loads Carried by the Tool During Friction Stir Welding," J. Mater. Eng. Perform., **18**, pp. 339–350.
[18] Kumar, K., and Satish, V., 2008, "On the Role of Axial Load and the Effect of Interface Position on the Tensile Strength of a Friction Stir Welded Aluminium Alloy," Mater. Des., **29**, pp. 791–797.
[19] Ericsson, M., and Sandstrom, R., 2003, "Influence of Welding Speed on the Fatigue of Friction Stir Welds and Comparison with MIG and TIG," Int. J. Fatigue, **25**, pp. 1379–1387.
[20] James, M. N., Hattingh, D. G., and Bradley, G. R., 2003, "Weld Tool Travel Speed Effect on Fatigue Life of Friction Stir Welds in 5083 Aluminum," Int. J. Fatigue, **25**, pp. 1389–1398.
[21] Shusheng, D., Xinqi, Y., Guohom, L., and Bo, J., 2006, "Comparative Study on Fatigue Properties Between AA2024-T4 Friction Stir Welds and Base Materials," Mater. Sci. Eng. A, 435–436, pp. 389–395.
[22] Dickerson, T. L., and Przydatek, J., 2003, "Fatigue of Friction Stir Welds in Aluminium Alloys That Contain Root Flaws," Int. J. Fatigue, **25**, pp. 1399–1409.
[23] Fratini, L., Pasta, S., and Reynolds, A. P., 2009, "Fatigue Crack Growth in 2024-T351 Friction Stir Welded Joints: Longitudinal Residual Stress and Microstructural Effects," Int. J. Fatigue, **31**, pp. 495–500.
[24] Nishihara, T., 2006, "Development of Simplified FSW Tool," Proceedings of the 6th International Symposium on Friction Stir Welding, Saint Sauveur, Quebec, Canada.